Using and Abusing Equivariance

Tom Edixhoven Attila Lengyel Jan C. van Gemert
Delft University of Technology

Abstract

In this paper we show how Group Equivariant Convolutional Neural Networks use subsampling to learn to break equivariance to the rotation and reflection symmetries. We focus on the 2D rotations and reflections and investigate the impact of the broken equivariance on network performance. We show that a change in the input dimension of a network as small as a single pixel can be enough for commonly used architectures to become approximately equivariant, rather than exactly. We investigate the impact of networks not being exactly equivariant and find that approximately equivariant networks generalise significantly worse to unseen symmetries compared to their exactly equivariant counterparts. However, when the symmetries in the training data are not identical to the symmetries of the network, we find that approximately equivariant networks can relax their equivariance constraints, matching or outperforming exactly equivariant networks on common benchmarks.

1. Introduction

Nature contains a lot of symmetries [18] and networks used for computer vision have been shown to benefit greatly from prior knowledge of these symmetries. Most notably, the introduction of the convolution operator resulted in the creation of *Convolutional Neural Networks* (CNN) [29], form a backbone of many computer vision applications. Convolutions are *equivariant* to the translation symmetry [22], meaning that if an object in the input image is shifted, the output of the convolution is shifted equally. Due to translation equivariance, networks no longer have to explicitly learn to recognise objects at all possible locations, as the knowledge that location plays no role is embedded into the network.

Images, however, regularly contain other relevant symmetries for which CNNs are not equivariant. Take for example the field of histopathology, which entails the microscopic examination of organic tissue. In histopathology, the rotational orientation of the tissue is arbitrary [24]. A network that varies its output when the input is rotated is therefore a cause for uncertainty. More formally, the output of the network should be *invariant* to rotation, meaning that the output should not change when the input is rotated.

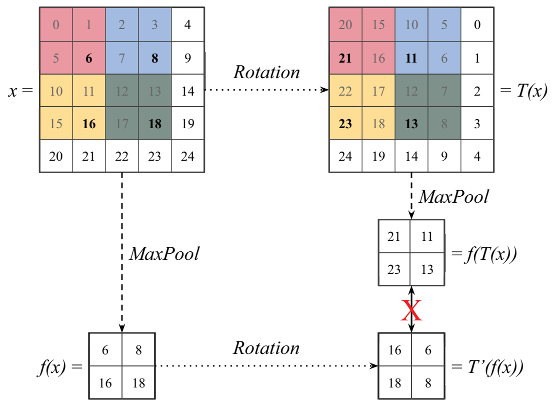

Figure 1: Example of how subsampling can break equivariance. Dotted arrows indicate a *Rotation* and the dashed arrows indicate a *MaxPool* subsampling layer with a kernel size and stride of 2. The locations where *MaxPool* applies its pooling are coloured. One can see that $f(T(x))$ and $T'(f(x))$ contain completely different numerical values, breaking equivariance.

A major innovation in equivariance for computer vision was the introduction of *Group Equivariant Convolutions* (GEC) [5], which made it possible for CNNs to guarantee equivariance or invariance to a finite group of discrete transformations, also referred to as a *symmetry group*. Using GECs instead of standard convolutions to create a network yields a *Group Equivariant Convolutional Neural Network* (GCNN). Due to the group equivariant properties of GECs, GCNNs guarantee that the network output does not change when the input is rotated.

In this paper, we explore subsampling layers in GCNNs that allow the networks to break their guarantee of equivariance. Consider the *MaxPool* subsampling layer in Figure 1. The feature map resulting from first rotating and then subsampling contains completely different numerical values than the result of first subsampling and then rotating, and as such the *MaxPool* layer is not equivariant to rotations. Whether a subsampling layer breaks equivariance is dependent on the width and height of the input, also referred to as *input dimension*. Including a subsampling layer that breaks equivariance in a GCNN will void the entire GCNN's guarantee of equivariance. However, subsampling layers are deemed almost essential for computer vision models and are used in nearly all GCNNs and modern CNNs. Typically, no distinction is made between GCNNs that do or do not contain subsampling layers that break equivariance. In this work, we show why a distinction should be made. We refer to networks in which subsampling layers break the guarantee of equivariance as *approximately equivariant* and networks in which the guarantee is not broken are referred to as *exactly equivariant*.

We offer the following contributions. We give a formal definition of exact equivariance under subsampling and can analyse when equivariance is broken. We show that approximately equivariant networks learn to become less equivariant and as a result generalise significantly worse to unseen symmetries compared to their exact counterparts. We show that slightly changing the input dimensions is often enough to make a network exactly equivariant rather than approximately equivariant.

2. Related Work

2.1. Equivariance in Deep Learning

CNNs are able to learn to become equivariant from data [12, 28]. However, this does not guarantee equivariance to the symmetries in the data and results in a redundancy in the filters of the network. For example, the network learns one filter to detect horizontal lines and a separate one to detect vertical lines, rather than a single filter to detect lines. Much work has been written about how to efficiently teach networks equivariance to relevant symmetries during training, either by separating symmetry weights from filter weights [16, 23, 40], using contrastive learning [4, 11] or using marginal likelihood [34, 35]. However, while these methods significantly increase a network's ability to become equivariant, they do not guarantee it. Each method relies on the network learning the equivariance from the training data. However, the training data seldom guarantees a full and uniformly distributed representation of the relevant symmetries. These possible biases in the training data can then propagate into biases in the network. This can be cause for concern, as biased networks make systematic errors due to faulty assumptions about the data.

If the symmetry group for which a network needs to be equivariant is known, a common solution is to encode the symmetries into the network as prior knowledge using Group Equivariant Convolutions (GECs) [5]. GECs are equivariant to finite set of discrete transformations defined in a symmetry group. Filter weights are then shared within the GECs according to the transformations. Because the GECs include all transformations from their symmetry group, GECs guarantee equivariance to the symmetries, regardless of biases in the training data.

The introduction of GECs kickstarted much follow-up work, including extensions from 2D planes to 3D manifolds [6, 7, 37] and the generalisation from discrete to continuous transformations using Lie algebra [8] or other means [32]. In this work, we focus on using GECs to become equivariant and invariant to the 2D roto-translation group, as the group has been proven to be useful in the field of histopathology [2, 24, 36] and processing satellite data [13, 25]. The 2D roto-translation groups consists of all rotations and translations in a 2-dimensional space. However, GECs are equivariant to discrete transformations and the 2D roto-translation group is continuous. Therefore, we make our networks equivariant to the *p4*-group [5], consisting of all compositions of translations and $90°$ rotations, meaning that the networks are also equivariant to rotations of $180°$ and $270°$.

2.2. Breaking Equivariance

While CNNs are generally regarded to be translation equivariant, a plethora of work has shown that this is not completely the case. Convolutions and pooling with a stride larger than 1 have been shown to break translation equivariance [3, 15, 38, 39]. CNNs have also been shown to be able to learn absolute positions, thereby breaking the translation equivariance [19]. This is important to note, as Group Equivariant Convolutions assume that standard convolutions are translation equivariant to prove their equivariance to other transformations. Preventing networks from breaking their roto-translation equivariance has been investigated for reconstruction learning by introducing a group equivariant subsampling layer [38]. This method however requires additional compute and the effects on classification has not been investigated, where invariance is often more desirable than equivariance. In this work, we extend the current literature by investigating the influence of subsampling on roto-translation equivariance for classification.

The general proof for equivariance in GCNNs holds when the convolution convolves over the entire input. However, networks often unknowingly break this restriction. Pooling and strided convolutions are often used to aggregate local information and increase the receptive field of a network [17]. The combination of stride, input size and kernel size in subsampling layers can result in different values from the input feature map being sampled, resulting in approximate equivariance rather than exact equivariance [30]. While it might seem like a minute detail, we find that it causes GCNNs to underperform relative to other equivariant networks in related works. Examples of rotation equivariant GCNNs exhibiting unexpected behaviour can be found in [1, 26]. In this work, we show that we can guarantee equivariance for GCNNs by introducing a relatively simple restriction on the combination of input size, kernel size and stride.

2.3. Relaxing Equivariant Constraints

Recent work has shown the possible benefits of relaxing equivariant constraints, showing that networks can gain performance by allowing them to learn to become less equivariant [31, 33]. This is relevant for our work, since being approximately equivariant seems to allow networks to relax their own equivariant constraints. Similarly to the aforementioned works, our solution also enables the user to make a conscious decision whether to relax the equivariant constraints on a network.

3. How subsampling breaks equivariance

In this section we provide a more formal introduction to equivariance and Group Equivariant Convolutions (GConvs). We will then show a simple network configuration including a subsampling operation that breaks the equivariance property of GConvs. Subsequently we introduce a constraint on the network configuration that does guarantee exact equivariance under subsampling, and provide a proof for rotations and mirroring.

3.1. Group Equivariant Convolutions

A network f is equivariant to transformation T, when the output of f on input x changes predictably when x is transformed by T. More formally, there exists a transformation T' for which the following equality holds:

$$f(T(x)) = T'(f(x)). \tag{1}$$

GCNNs are equivariant to a set of transformations defined in a symmetry group G, where in practice the transformations are stored in an additional group dimension in the feature maps. In the case of the *p4*-group, T' consists of a rotation in the spatial dimensions and permutation of the group dimension on the feature map. Invariance to T is achieved by applying a coset pooling operation on the group dimension, such that the final representation satisfies

$$f(T(x)) = f(x). \tag{2}$$

As such, invariance is considered a special case of equivariance.

3.2. Exact and Inexact Equivariance

From Equation 1 and the cyclic permutation defined by T' it follows that the feature maps of an exactly equivariant GCNN should contain the same numerical values regardless of the applied rotation T to the input. However, layers that perform subsampling on the input can introduce numerical differences depending on the input transformation, resulting in the network architecture no longer being exactly equivariant, as we will now demonstrate.

Let x be a rectangular input of dimension $i = 5$, f a network consisting of a single *MaxPool* layer with kernel size $k = 2$ and stride $s = 2$, and T a clockwise rotation of $90°$. As the reference point of the 2D subsampling operation is always defined at the $(0, 0)$ index of the input, applying T results in the sampling indices being shifted by a single pixel from the perspective of the *MaxPool* layer. Subsequently, $T'(f(x))$ and $f(T(x))$ contain different numerical values, as shown in Figure 1. To guarantee exact equivariance we therefore need to ensure that the same indices are sampled, irrespective of the order in which the sampling operation and rotation are applied. Our proposed solution is simple as it does not require any modifications to the network architecture and relies purely on setting appropriate input dimensions to the network. For comprehensibility, we focus on the case of square inputs $\in \mathbb{R}^{i \times i}$ and an arbitrary kernel size k and stride s, but the proof can be readily extended to rectangular inputs $\in \mathbb{R}^{j \times i}$.

A GCNN is exactly equivariant to rotations of multiples of $90°$ if the following equation holds for all layers in the network:

$$(i - k) \mod s = 0. \tag{3}$$

We prove that Equation 3 is a necessary condition for exact equivariance to $90°$ rotations by asserting that the sampled indices for a given output index remain the same under rotation. We define a new function called index, that returns the indices of the input values used by a convolutional or pooling layer to calculate the value located at index (x, y) in the output:

$$\text{index}\left(\begin{bmatrix} x \\ y \end{bmatrix}\right) = \left[\begin{bmatrix} sx \\ sy \end{bmatrix}, \begin{bmatrix} sx + k - 1 \\ sy + k - 1 \end{bmatrix}\right]. \tag{4}$$

Here s is the stride used for subsampling and k represents the kernel size. The output of the function is a square patch, denoted as $[\vec{u}, \vec{v}]$, where $\vec{u}$ and $\vec{v}$ represent the indices of the top left and bottom right corner, respectively. The sampled indices include all integer tuples within this patch. We also introduce the function R, which takes an index (x, y) as input and returns the indices rotated $90°$ counterclockwise:

$$R_n\left(\begin{bmatrix} x \\ y \end{bmatrix}\right) = \begin{bmatrix} y \\ n - 1 - x \end{bmatrix}, \tag{5}$$

where n indicates the width and height of the feature map in which the index (x, y) is located. We further generalise Equation 5 to an input patch $[\vec{u}, \vec{v}]$ rather than a single coordinate, resulting in Equation 6:

$$R_n\left([\vec{u},\vec{v}]\right) = R_n\left(\left[\begin{bmatrix}x_1\\y_1\end{bmatrix},\begin{bmatrix}x_2\\y_2\end{bmatrix}\right]\right) = \left[\begin{bmatrix}y_1\\n-1-x_2\end{bmatrix},\begin{bmatrix}y_2\\n-1-x_1\end{bmatrix}\right] \tag{6}$$

In the resulting output coordinates x_1 and x_2 get interchanged due to the counterclockwise rotation of the patch: the top left corner becomes the bottom left corner, while the bottom right corner becomes the top right corner.

Given that our layer takes a feature map with a width and height of i as input, we can write the width and height of the output feature map as

$$o = \lfloor\frac{i-k}{s}\rfloor + 1. \tag{7}$$

For a layer to be exactly equivariant, determining the sampled indices and then rotating should return the same result as rotating first and then determining the sampled indices, which we can formally denote as

$$\text{index}\left(R_o\left(\begin{bmatrix}x\\y\end{bmatrix}\right)\right) = R_i\left(\text{index}\left(\begin{bmatrix}x\\y\end{bmatrix}\right)\right). \tag{8}$$

To solve the left-hand side, we substitute Equation 5 into Equation 4, yielding

$$\begin{aligned}\text{index}\left(R_o\left(\begin{bmatrix}x\\y\end{bmatrix}\right)\right) &= \\ \text{index}\left(\begin{bmatrix}y\\\lfloor\frac{i-k}{s}\rfloor - x\end{bmatrix}\right) &= \\ \left[\begin{bmatrix}sy\\s\lfloor\frac{i-k}{s}\rfloor - sx\end{bmatrix},\begin{bmatrix}sy+k-1\\s\lfloor\frac{i-k}{s}\rfloor - sx + k - 1\end{bmatrix}\right]&.\end{aligned} \tag{9}$$

The same can be done for the right-hand side, by substituting Equation 4 into Equation 6, resulting in

$$\begin{aligned}R_i\left(\text{index}\left(\begin{bmatrix}x\\y\end{bmatrix}\right)\right) &= \\ R_i\left(\left[\begin{bmatrix}sx\\sy\end{bmatrix},\begin{bmatrix}sx+k-1\\sy+k-1\end{bmatrix}\right]\right) &= \\ \left[\begin{bmatrix}sy\\i-k-sx\end{bmatrix},\begin{bmatrix}sy+k-1\\i-1-sx\end{bmatrix}\right]&.\end{aligned} \tag{10}$$

Substituting Equations 9 and 10 into Equation 8, we find two equations

$$s\lfloor\frac{i-k}{s}\rfloor - sx = i-k-sx, \tag{11}$$

$$s\lfloor\frac{i-k}{s}\rfloor - sx + k - 1 = i-1-sx. \tag{12}$$

Removing duplicate terms yields a single equation

$$s\lfloor\frac{i-k}{s}\rfloor = i-k, \tag{13}$$

which can be simplified to Equation 3. As Equation 3 holds for a rotation of 90°, it automatically holds for rotations of 180° and 270°, as these can be composed using multiple rotations of 90°. We provide a similar proof for mirroring in the supplementary material.

3.3. Measuring Equivariance and Invariance

We evaluate the exactness of the equivariance property of GConvs both in terms of their measured invariance and equivariance.

Measuring equivariance Since in GConvs both T and T' are known transformations, feature maps $f(T(x))$ and $T'(f(x))$ can be computed independently. We can thus define the equivariance error in terms of the Mean Squared Error (MSE) between the two feature maps:

$$\begin{aligned}\epsilon &= \text{MSE}(f(T(x)), T'(f(x))) \\ &= \frac{1}{ijk}\sqrt{\sum_{i,j,k}|f(T(x))_{ijk} - T'(f(x))_{ijk}|^2},\end{aligned} \tag{14}$$

where i and j sum over the spatial dimensions of the feature map and k sums over the group dimension. The equivariance error can be evaluated at any GConv layer in the network.

Measuring invariance To measure the invariance of the network output after coset pooling we apply a range of rotations in $[0°, 360°)$ to the test set and report the test accuracy for each set separately. However, rotating an image by degrees other than multiples of 90° introduces artefacts at the corners of the image, as shown in Figure 2 (left). These artifacts have an additional detrimental effect on the network's performance. To ensure we only measure the performance drop due to rotation, we apply a *CircleCrop*, which sets all values whose coordinates are not inside the largest possible inscribed circle to 0, as visualised in Figure 2 (right). To prevent any domain shift between the train and test set, we apply *CircleCrop* during both training and evaluation. *Nearest Neighbour Interpolation* also affected model performance and so all rotations are performed using *Bilinear Interpolation*.

4. Experiments

4.1. Breaking Equivariance

In this subsection, we show how networks can learn to break their equivariance to improve their performance, and demonstrate that they in practice do so on commonly used classification datasets.

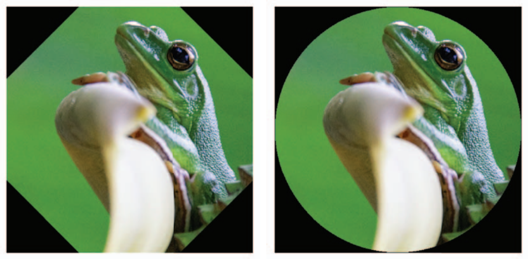

Figure 2: **Left:** Rotated input without *CircleCrop*. **Right:** Rotated input with *CircleCrop*. Without *CircleCrop* the rotation is distinctive.

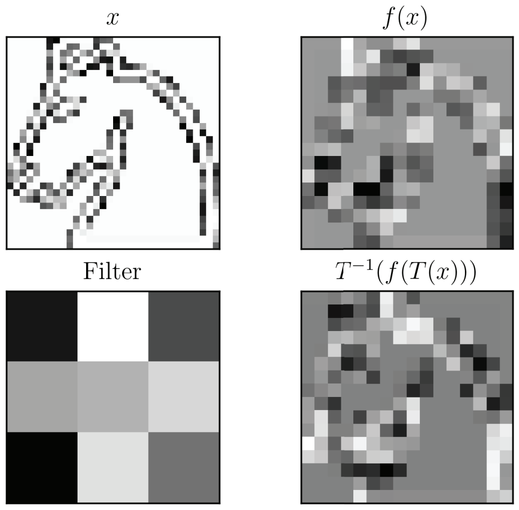

Figure 3: A subsampling Group Equivariant net f that is equivariant to the 90° rotation transformation T can learn a filter that returns almost inverted values for $f(x)$ and $T^{-1}(f(T(x)))$, while these outputs should be identical in theory. Because the outputs are not equal, a network using the filter f can perfectly distinguish between x and $T(x)$.

Can GCNNs break equivariance? If a GCNN is truly invariant, it should be unable to distinguish between an input x and $T(x)$, where T is a 90° rotation. We challenge this assumption by explicitly training a simple GCNN to differentiate between the two input samples x and $T(x)$. We construct a network consisting of (i) a GConv layer with $k = 3$, $s = 2$, 1 output channel and a padding of 1; (ii) a global average pooling layer over the spatial dimensions; (iii) a coset max pooling layer over the group dimension to obtain a rotation invariant representation; and (iv) a fully connected layer with two output features.

We define an input $x_1 \in \mathbb{R}^{32\times 32}$ as shown in the top left of Figure 3 and train the network on x_1 and $T(x_1)$. We find that the network can perfectly distinguish between the two samples as shown by the feature maps in the right column in Figure 3. This demonstrates that the network is not invariant, despite the pooling operation on the group dimension. We furthermore define a second input $x_2 \in \mathbb{R}^{33\times 33}$ and repeat the experiment. The network is not able to distinguish between x_2 and $T(x_2)$, showing that the same network architecture is exactly invariant for inputs in $\mathbb{R}^{33\times 33}$, while not being invariant for inputs in $\mathbb{R}^{32\times 32}$. This is in line with our findings in Section 3.2, as for $k = 3$, $s = 2$ and $i = 33$

$$(i - k) \mod s = (33 - 3) \mod 2 = 0$$

holds, whereas for $i = 32$

$$(i - k) \mod s = (32 - 3) \mod 2 = 1 \neq 0$$

does not. Thus, GCNNs can break equivariance.

Breaking equivariance on common benchmarks. We have shown that when the objective of a GCNN is to break its equivariance, it will do so if possible. However, the question remains whether a network will also learn to do so when breaking equivariance is not explicitly the objective.

We first investigate the ImageNet [9] classification problem. We create a rotation equivariant ResNet18 [14] by substituting standard convolutions with *p4*-convolutions. The network width is divided by $\sqrt{4}$ to keep the number of parameters approximately equal to a standard ResNet18 and the input images are kept at their original 224×224 size. Training is performed for 90 epochs using the default training settings, i.e. SGD with momentum 0.9 and learning rate 0.1, which is step-wise reduced by a factor 0.1 every 30 epochs. The network is trained to classify the standard ImageNet classes, so there is no explicit objective to distinguish between rotations. Throughout training we monitor the equivariance error as defined in Equation 14 after the first layer and each of the four ResNet stages. The measured equivariance errors are shown in Figure 4a. We observe that initially all equivariance errors drop to a more or less constant value, and upon decreasing the learning rate at epoch 30 the equivariance error further drops in most stages in the network. However, the error at the last stage of the network increases rapidly, finally plateauing at a value higher than after random initialization.

Secondly, we look at the PatchCamelyon dataset [36]. This dataset is interesting because it is pathology data, which, unlike ImageNet images, should not contain any dominant rotation bias. We use a similar setup to our previous ImageNet experiment, but we replace the ResNet18 with a ResNet44. The network width is decreased to obtain an approximately equal number of parameters as in the architecture used by Veeling *et al.* [36] when evaluating on PatchCamelyon. The results on PatchCamelyon can be found in Figure 4b. As the first layer and the first stage both

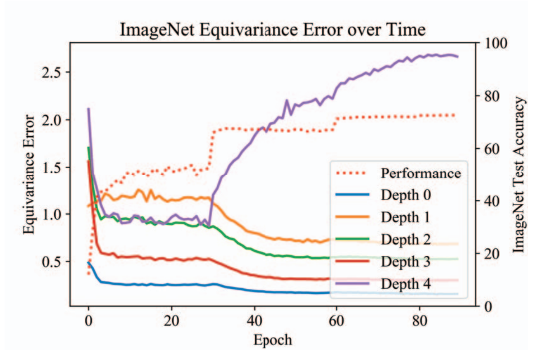

(a)

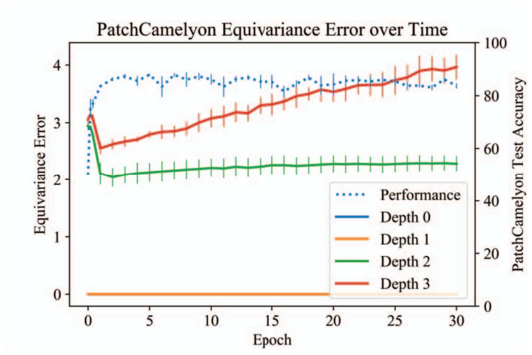

(b)

Figure 4: The measured equivariance error at different depths in a $p4$-ResNet, trained on ImageNet (a) and PatchCamelyon (b), respectively. The classification accuracy is indicated as a dotted red line. The equivariance error in the final layer increases throughout training, indicating that the network is learning to become less equivariant, even when trained on the rotation invariant PatchCamelyon dataset.

have a stride of 1, the equivariance error is a constant 0 at the first two depth measurements. The other two stages show a similar behavior as in the ImageNet experiment, with a rapid decrease in the initial part of the training and a gradual decrease in the final stage throughout the remainder of the training run. Interestingly, even though PatchCamelyon is a rotation invariant dataset by definition, the network still learns to break its equivariance.

We can thus conclude that a network that is equivariant to rotations can learn to abuse its approximate equivariance to become less equivariant to rotations. This occurs both when the network is trained on ImageNet, a dataset which contains only a limited amount of rotations and a clear upright orientation bias, as well as the PatchCamelyon dataset which should be rotation invariant by definition. A network learning differences between rotations in a rotation invariant setting is cause for concern, as the rotations are arbitrary and therefore should not contain any relevant information.

4.2. Impact of Exact Equivariance

Performance on unseen rotations Due to the discrete nature of GCNNs, it is impossible to include all continuous rotations in the discrete group. Thus, it is important to generalise well to rotations that are not part of the group dimension. To compare how well approximately and exactly equivariant networks generalise to unseen rotations, we perform a controlled experiment on the MNIST [10] dataset of handwritten digits. Since MNIST contains limited rotations due to slanted handwriting, we are able to control what rotations are included during training and testing by transforming the data.

For this experiment, we use the Z2CNN and P4CNN architectures introduced by Cohen *et al*. [5]. The Z2CNN consists of 6 layers of 3×3 convolutions, followed by a single 4×4 convolutional layer, each layer consisting of 20 channels. Each layer is followed by a ReLU activation and batch normalisation layer. A dropout layer with $p = 0.3$ is added after layers 1 through 5, and a max-pooling layer with a stride of 2 after the second layer. The convolutional part is followed by a global spatial average-pooling layer, and lastly, a fully connected layer. The P4CNN architecture is created by substituting standard convolutions with *p4*-convolutions and introducing a group coset max-pooling layer before the fully connected layer. To keep the number of parameters of Z2CNN and P4CNN approximately equal, the number of channels in P4CNN is divided by $\sqrt{4}$. We use the default input size of 28×28 for exact equivariance, and input sizes 27×27 and 29×29 for approximate equivariance. The results are averaged over 10 runs with different random seeds. The models are trained for 50 epochs using Adam [20] and an initial learning rate of 0.01, which is halved every 10 epochs.

The results in Figure 5 show the performance of a model trained on MNIST and evaluating on RotMNIST, a uniformly rotated version of MNIST. An exactly equivariant network will significantly outperform approximate counterparts on rotated samples. All the *p4*-equivariant networks still outperform the Z2CNN baseline. We also observe a much higher standard deviation in the performance of the approximately equivariant networks. The performance increase of Z2CNN at $180°$ can be attributed to the rotational symmetries in the MNIST dataset. The $0, 1$ and 8 classes stay roughly identical when rotated $180°$.

To further evaluate network generalisability to unseen rotations, we create two new versions of RotMNIST with biased rotation transformations. The rotation of each training digit is sampled from a normal distribution. Both datasets use a mean rotation of $45°$, one has a standard devi-

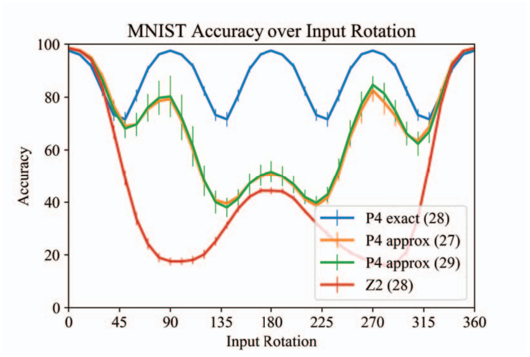

Figure 5: The equivariance of a network can be evaluated by explicitly applying the transformation on the test set. When the training contains no data augmentations, an exactly equivariant network generalises significantly better than its approximate counterpart.

ation of $20°$ and the other of $40°$. We then train the networks on these biased training sets and evaluate them on a test set with uniform rotations. The results in Figure 6 show that, similarly to training on non-rotated data, the exactly equivariant network generalises noticeably better than the others. The exactly equivariant network almost becomes invariant to rotations in general, while all other networks exhibit a significant drop in performance on rotations that are not in the training data. Since the transformation distributions in the training data are often unknown, it is important to generalise to instances of the transformation that are not in the training data.

We further evaluate the impact of exact and approximate equivariance on common benchmark datasets, where we differentiate between datasets with and without rotational symmetries. Datasets with rotations include *Flowers102* [27], where many classes have a rotationally symmetric shape, and *PatchCamelyon* [36], which is completely invariant to rotation. Datasets without rotational symmetries include *Cifar10*, *Cifar100* [21] and *ImageNet* [9]. We evaluate for unseen rotations by rotating the test set by multiples of $90°$ and averaging the performance over the four rotations. To achieve exact and approximate p4-equivariance, we change the input size of the network, such that equation 3 holds for all layers in the network. The results are shown in Table 2. The approximately equivariant networks are outperformed by the exactly equivariant networks in all cases. The difference is most significant for datasets that contain limited rotations, i.e. *Cifar10*, *Cifar100* and *ImageNet*, as here the model is not able to learn the symmetries from data. Both the exact and inexact networks outperform the baseline CNN by a large margin, showing that in general inexact equivariance is a beneficial property.

Model	Equivar.	MNIST	RotMNIST
Z2CNN	- (28)	98.47 ± 0.17	91.60 ± 1.25
P4CNN	Approx (27)	98.52 ± 0.26	96.92 ± 0.27
P4CNN	Exact (28)	97.69 ± 0.17	96.89 ± 0.21
P4CNN	Approx (29)	98.42 ± 0.25	96.87 ± 0.25

Table 1: Network accuracy denoted as mean $\pm$ standard deviation on MNIST and RotMNIST test sets. The standard deviation is calculated using a 100 runs with different seeds. The equivariance column indicates whether the network is exactly or approximately equivariant and contains the network input size in parentheses.

Performance on seen rotations For the performance on rotations that are included in the training data, also referred to as seen rotations, we first evaluate MNIST and RotMNIST using P4CNN and Z2CNN as in Section 4.2. We report the mean and standard deviations of the test accuracies over 100 run with different random seeds in Table 1. On MNIST the exactly equivariant network exhibits a performance drop between 0.65% and 0.91% compared to its approximately equivariant counterparts, which is confirmed to be statistically significant, as shown in the supplementary material. On RotMNIST the exact network performs identically to the approximate networks, as the approximate networks are able to learn to become invariant from the transformations found in the training data.

To evaluate for seen rotations on common classification benchmarks we compute the model accuracy on the default test set. The benchmark results can be found in Table 2. The exactly equivariant networks are generally matched or outperformed by their approximately equivariant counterparts, even on datasets containing rotational symmetries. This seems to indicate that there lies value in relaxing the equivariant constraints of networks. Furthermore, both *p4*-equivariant networks outperform their *z2*-equivariant counterparts, even when the dataset is not known for containing many rotational symmetries. This could indicate that the improvements from the group equivariant architecture might not be solely from equivariance, but could also originate from other traits of GCNNs. Other possible explanations are the increase in computations or the amount of gradients a GCNN uses compared to a standard CNN.

5. Conclusion

In this work, we show that Group Equivariant Convolutions [5] can and do learn to break their equivariance towards the 2D rotations in common use cases. We prove theoretically and empirically that changing the input size of the network is sufficient to prevent a network from breaking its equivariance. We find that exactly equivariant networks

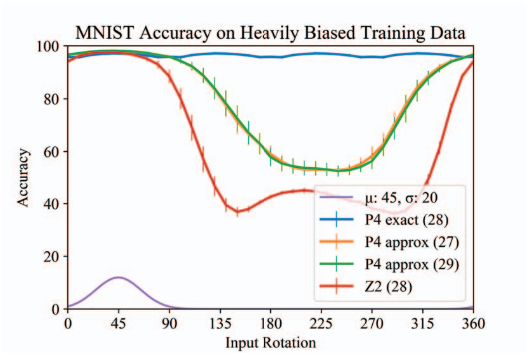

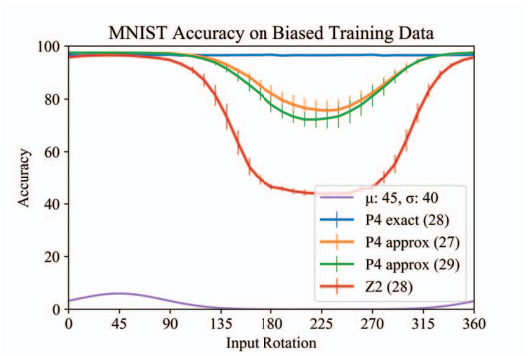

Figure 6: An exactly equivariant network generalises significantly better to unseen rotations in case of a rotation bias in the training data. The rotation angles of the training set are sampled from a normal distribution $\mathcal{N}(\mu, \sigma)$, visualised at the bottom of each plot. The plot on the left shows the performance on a biased distribution with $\sigma = 20$. The plot the right shows the performance on a biased distribution with $\sigma = 40$, which is less severe but still significant.

Dataset	**Model**	**Unseen rotations**			**Seen rotations**		
		Approx. $p4$	Exact $p4$	Standard	Approx. $p4$	Exact $p4$	Standard
Flowers102	ResNet-18	83.32 ± 1.21	$\mathbf{86.65 \pm 1.41}$	68.78 ± 0.29	86.28 ± 1.32	$\mathbf{86.65 \pm 1.41}$	82.18 ± 0.53
PCam	ResNet-44	86.66 ± 0.72	$\mathbf{87.40 \pm 0.71}$	82.43 ± 1.71	$\mathbf{87.52 \pm 1.20}$	87.40 ± 0.71	85.35 ± 1.04
CIFAR10	ResNet-44	79.19 ± 0.47	$\mathbf{93.41 \pm 0.09}$	52.68 ± 0.11	$\mathbf{94.80 \pm 0.21}$	93.41 ± 0.09	93.20 ± 0.11
CIFAR100	ResNet-44	58.82 ± 0.36	$\mathbf{72.28 \pm 0.40}$	38.62 ± 0.16	$\mathbf{75.00 \pm 0.52}$	72.28 ± 0.40	70.09 ± 0.28
ImageNet	ResNet-18	60.01	**72.55**	48.10	72.48	**72.55**	70.00

Table 2: Test accuracies of ResNet models on seen and unseen rotations of common classification benchmarks. Exactly equivariant networks perform significantly better on unseen rotations, especially on datasets containing no rotation symmetries, i.e. CIFAR and ImageNet. Approximate networks are able to relaxe equivariance constraints and perform better on seen rotations. All *p4*-equivariant networks outperform the standard CNN.

generalise significantly better to unseen rotations than their approximately equivariant counterparts, but that when the training data contains all relevant rotations there is no significant difference. We find that due to broken translation equivariance, the rotation equivariance of GCNNs is also broken. It could prove interesting to further investigate the effect of making networks truly equivariant to translations [3] on equivariance to other symmetries.

Interestingly, we also find results that suggest equivariant networks offer performance increases to datasets that do not contain the relevant transformations, suggesting that using GCNNs might offer benefits other than equivariance to certain symmetries. Furthermore, we find that relaxing equivariant constraints can be beneficial for network performance. However, relaxing equivariant constraints also allows networks to become biased towards the distribution of transformations in the training data.

6. Limitations and Future Work

The symmetries our method applies to are limited to rotations and reflections. While these symmetries are relevant, future work can include other symmetries, or more rotations in the group dimension, such as all rotations of 45 °, rather than rotations of $90°$.

We found experimentally that padding has a large influence on how well a GCNN generalises to unseen rotations, similar to CNNs [19]. We found no explanation, but believe it is worth further investigating.

Section 4.1 suggests that equivariant layers are more desirable at some depths than others, since the equivariance error drops at some depths and rises at others. An interesting future work would be making a robust analysis of desirability of equivariance at different depths in a network.

Finally, we welcome further investigations of our results on PatchCamelyon, where we found that the approximately equivariant network learned to break its equivariance to increase performance, even on a problem supposedly invariant to rotation. With the rise of relaxed equivariant constraints [31, 33], an interesting question to ask would be whether we are actually achieving better performance or simply exploiting unknown biases in data or in the network.

Acknowledgements. This project is (partly) financed by the Dutch Research Council (NWO) (project VI.Vidi.192.100).

References

[1] Piyush Bagad, Floor Eijkelboom, Mark Fokkema, Danilo de Goede, Paul Hilders, and Miltiadis Kofinas. C-3PO: Towards rotation equivariant feature detection and description. In *3rd Visual Inductive Priors for Data-Efficient Deep Learning Workshop*, 2022. 3

[2] Erik J Bekkers, Maxime W Lafarge, Mitko Veta, Koen A J Eppenhof, Josien P W Pluim, and Remco Duits. Roto-Translation Covariant Convolutional Networks for Medical Image Analysis. In Alejandro F. Frangi, Julia A. Schnabel, Christos Davatzikos, Carlos Alberola-López, and Gabor Fichtinger, editors, *Medical Image Computing and Computer Assisted Intervention – MICCAI 2018*, pages 440–448. Springer International Publishing, 2018. 2

[3] Anadi Chaman and Ivan Dokmanic. Truly shift-invariant convolutional neural networks. In *Proceedings of the IEEE/CVF Conference on Computer Vision and Pattern Recognition (CVPR)*, pages 3773–3783, June 2021. 2, 8

[4] Ting Chen, Simon Kornblith, Mohammad Norouzi, and Geoffrey Hinton. A simple framework for contrastive learning of visual representations. In *International conference on machine learning*, pages 1597–1607. PMLR, 2020. 2

[5] Taco Cohen and Max Welling. Group equivariant convolutional networks. In Maria Florina Balcan and Kilian Q. Weinberger, editors, *Proceedings of The 33rd International Conference on Machine Learning*, volume 48 of *Proceedings of Machine Learning Research*, pages 2990–2999, New York, New York, USA, 2016. PMLR. 1, 2, 6, 7

[6] Taco S. Cohen, Maurice Weiler, Berkay Kicanaoglu, and Max Welling. Gauge equivariant convolutional networks and the icosahedral cnn. In *International Conference on Machine Learning*, 2019. 2

[7] Pim De Haan, Maurice Weiler, Taco Cohen, and Max Welling. Gauge equivariant mesh cnns: Anisotropic convolutions on geometric graphs. *arXiv preprint arXiv:2003.05425*, 2020. 2

[8] Nima Dehmamy, Robin Walters, Yanchen Liu, Dashun Wang, and Rose Yu. Automatic symmetry discovery with lie algebra convolutional network. In M. Ranzato, A. Beygelzimer, Y. Dauphin, P.S. Liang, and J. Wortman Vaughan, editors, *Advances in Neural Information Processing Systems*, volume 34, pages 2503–2515. Curran Associates, Inc., 2021. 2

[9] Jia Deng, Wei Dong, Richard Socher, Li-Jia Li, Kai Li, and Li Fei-Fei. Imagenet: A large-scale hierarchical image database. In *2009 IEEE Conference on Computer Vision and Pattern Recognition*, pages 248–255, 2009. 5, 7

[10] Li Deng. The mnist database of handwritten digit images for machine learning research. *IEEE Signal Processing Magazine*, 29(6):141–142, 2012. 6

[11] Alexandre Devillers and Mathieu Lefort. Equimod: An equivariance module to improve self-supervised learning. *arXiv preprint arXiv:2211.01244*, 2022. 2

[12] Jonas Geiping, Micah Goldblum, Gowthami Somepalli, Ravid Shwartz-Ziv, Tom Goldstein, and Andrew Gordon Wilson. How much data are augmentations worth? an investigation into scaling laws, invariance, and implicit regularization. *arXiv preprint arXiv:2210.06441*, 2022. 2

[13] Jiaming Han, Jian Ding, Nan Xue, and Gui-Song Xia. Redet: A rotation-equivariant detector for aerial object detection. In *Proceedings of the IEEE/CVF Conference on Computer Vision and Pattern Recognition (CVPR)*, pages 2786–2795, 2021. 2

[14] Kaiming He, Xiangyu Zhang, Shaoqing Ren, and Jian Sun. Deep residual learning for image recognition. In *Proceedings of the IEEE conference on computer vision and pattern recognition*, pages 770–778, 2016. 5

[15] Md Amirul Islam, Matthew Kowal, Sen Jia, Konstantinos G Derpanis, and Neil DB Bruce. Global pooling, more than meets the eye: Position information is encoded channel-wise in cnns. In *Proceedings of the IEEE/CVF International Conference on Computer Vision*, pages 793–801, 2021. 2

[16] Max Jaderberg, Karen Simonyan, Andrew Zisserman, et al. Spatial transformer networks. *Advances in neural information processing systems*, 28, 2015. 2

[17] Dong-Hwan Jang, Sanghyeok Chu, Joonhyuk Kim, and Bohyung Han. Pooling revisited: Your receptive field is suboptimal. In *Proceedings of the IEEE/CVF Conference on Computer Vision and Pattern Recognition*, pages 549–558, 2022. 2

[18] Iain G. Johnston, Kamaludin Dingle, Sam F. Greenbury, Chico Q. Camargo, Jonathan P. K. Doye, Sebastian E. Ahnert, and Ard A. Louis. Symmetry and simplicity spontaneously emerge from the algorithmic nature of evolution. *Proceedings of the National Academy of Sciences*, 119(11):e2113883119, 2022. 1

[19] Osman Semih Kayhan and Jan C van Gemert. On translation invariance in cnns: Convolutional layers can exploit absolute spatial location. In *Proceedings of the IEEE/CVF Conference on Computer Vision and Pattern Recognition*, pages 14274–14285, 2020. 2, 8

[20] Diederik P. Kingma and Jimmy Ba. Adam: A method for stochastic optimization. *CoRR*, abs/1412.6980, 2014. 6

[21] Alex Krizhevsky, Geoffrey Hinton, et al. Learning multiple layers of features from tiny images. 2009. 7

[22] Alex Krizhevsky, Ilya Sutskever, and Geoffrey Hinton. Imagenet classification with deep convolutional neural networks. *Neural Information Processing Systems*, 25, 2012. 1

[23] Denis Kuzminykh, Daniil Polykovskiy, and Alexander Zhebrak. Extracting invariant features from images using an equivariant autoencoder. In Jun Zhu and Ichiro Takeuchi, editors, *Proceedings of The 10th Asian Conference on Machine Learning*, volume 95 of *Proceedings of Machine Learning Research*, pages 438–453. PMLR, 2018. 2

[24] Maxime W Lafarge, Erik J Bekkers, Josien PW Pluim, Remco Duits, and Mitko Veta. Roto-translation equivariant convolutional networks: Application to histopathology image analysis. *Medical Image Analysis*, 68:101849, 2021. 1, 2

[25] Joshua Mitton and Roderick Murray-Smith. Rotation equivariant deforestation segmentation and driver classification. *arXiv preprint arXiv:2110.13097*, 2021. 2

[26] Hanlin Mo and Guoying Zhao. Ric-cnn: Rotation-invariant coordinate convolutional neural network. *arXiv preprint arXiv:2211.11812*, 2022. 3

[27] Maria-Elena Nilsback and Andrew Zisserman. Automated flower classification over a large number of classes. In *Indian Conference on Computer Vision, Graphics and Image Processing*, 2008. 7

[28] Chris Olah, Nick Cammarata, Chelsea Voss, Ludwig Schubert, and Gabriel Goh. Naturally occurring equivariance in neural networks. *Distill*, 5, 2020. 2

[29] Keiron O'Shea and Ryan Nash. An introduction to convolutional neural networks. *arXiv preprint arXiv:1511.08458*, 2015. 1

[30] David W Romero, Erik J Bekkers, Jakub M Tomczak, and Mark Hoogendoorn. Attentive group equivariant convolutional networks. *arXiv preprint arXiv:2002.03830*, 2020. 2

[31] David W Romero and Suhas Lohit. Learning equivariances and partial equivariances from data. *arXiv preprint arXiv:2110.10211*, 2021. 3, 8

[32] Kai Sheng Tai, Peter Bailis, and Gregory Valiant. Equivariant transformer networks. In *International Conference on Machine Learning*, pages 6086–6095. PMLR, 2019. 2

[33] Tycho FA van der Ouderaa, David W Romero, and Mark van der Wilk. Relaxing equivariance constraints with non-stationary continuous filters. *arXiv preprint arXiv:2204.07178*, 2022. 3, 8

[34] Tycho F.A. van der Ouderaa and Mark van der Wilk. Learning invariant weights in neural networks. In James Cussens and Kun Zhang, editors, *Proceedings of the Thirty-Eighth Conference on Uncertainty in Artificial Intelligence*, volume 180 of *Proceedings of Machine Learning Research*, pages 1992–2001. PMLR, 2022. 2

[35] Mark van der Wilk, Matthias Bauer, ST John, and James Hensman. Learning invariances using the marginal likelihood. *Advances in Neural Information Processing Systems*, 31, 2018. 2

[36] Bastiaan S Veeling, Jasper Linmans, Jim Winkens, Taco Cohen, and Max Welling. Rotation equivariant cnns for digital pathology. In *Medical Image Computing and Computer Assisted Intervention–MICCAI 2018: 21st International Conference, Granada, Spain, September 16-20, 2018, Proceedings, Part II 11*, pages 210–218. Springer, 2018. 2, 5, 7

[37] Maurice Weiler, Patrick Forré, Erik Verlinde, and Max Welling. Coordinate independent convolutional networks–isometry and gauge equivariant convolutions on riemannian manifolds. *arXiv preprint arXiv:2106.06020*, 2021. 2

[38] Jin Xu, Hyunjik Kim, Thomas Rainforth, and Yee Teh. Group equivariant subsampling. *Advances in Neural Information Processing Systems*, 34:5934–5946, 2021. 2

[39] Richard Zhang. Making convolutional networks shift-invariant again. In *International conference on machine learning*, pages 7324–7334. PMLR, 2019. 2

[40] Allan Zhou, Tom Knowles, and Chelsea Finn. Meta-learning symmetries by reparameterization. *arXiv preprint arXiv:2007.02933*, 2020. 2